Fluorinated Boroxin-Based Anion Receptors for Lithium Ion Batteries: Fluoride Anion Binding, Ab Initio Calculations, and Ionic Conductivity Studies

Nanditha G. Nair,[†] Mario Blanco,*[,‡] William West,*[,§] F. Christoph Weise,[⊥] Steve Greenbaum,[⊥] and V. Prakash Reddy*[,†]

Department of Chemistry, Missouri University of Science and Technology, Rolla, Missouri 65409, Department of Chemistry, California Institute of Technology, Pasadena, California 91109, Jet Propulsion Laboratory, California Institute of Technology, Pasadena, California 91109, and Hunter College, City University of New York, New York 10021

Received: March 3, 2009; Revised Manuscript Received: April 3, 2009

Novel fluorinated boroxines, tris(2,6-difluorophenyl)boroxin (DF), tris(2,4,6-trifluorophenyl)boroxin (TF), and tris(pentafluorophenyl)boroxin (PF), have been investigated for potential applications in lithium ion batteries through fluoride anion binding, ab initio calculations, and ionic conductivity measurements. Structures of the fluorinated boroxines and boroxin−fluoride complexes have been confirmed by comparing their ^{19}F and ^{11}B NMR chemical shifts with those obtained by the DFT-GIAO method. The stoichiometry of the fluoride anion binding to these boroxines has been shown to be 1:1 using ^{19}F NMR and UV−vis spectroscopy. UV−vis spectroscopic studies show the coexistence of more than one complex, in addition to the 1:1 complex, for perfluorinated boroxin, PF. DFT calculations (B3LYP/6-311G**) show that the fluoride ion complex of DF prefers unsymmetrical, covalently bound structure (**7**) over the symmetrically bridged species (**10**) by 12.5 kcal/mol. Rapid equilibration of the fluoride anion among the three borons in these boroxines results in a single ^{19}F NMR absorption for all of the aromatic *ortho*- or *para*-fluorines at ambient temperature. The effect of these anion receptors on lithium ion conductivities was also explored for potential applications in dual ion intercalating lithium batteries.

Introduction

The state of the art electrolytes in the conventional lithium ion batteries are based on a variety of carbonate-based solvents and $LiPF_6$. Coordination of Lewis-basic carbonate solvents with lithium salts results in a decrease in lithium ion transference numbers. Further, reaction of $LiPF_6$ or related salts with traces of water in the electrolyte solvents releases Bronsted acids such as HF, which serve as initiators for the ring-opening polymerization of cyclic carbonate solvents and other undesirable effects including corrosion of cathode materials, which limits the specific energies obtainable from these batteries.

A rechargeable C−F cathode would be very desirable in terms of specific energy relative to conventional lithium ion transition metal oxide cathodes. However, there are numerous difficulties associated with reversible fluorination of carbon which relate to, to a large extent, the nature of the C−F bond. To date, all C−F cathodes, regardless of preparation conditions, are strictly nonrechargeable. Recently, a novel dual ion (Li^+, F^-) intercalating lithium fluoride battery has been developed using LiF as a low-molecular-weight electrolyte dissolved in nonaqueous solvents aided by boron-based anion receptors such as tris(pentafluorophenyl)borate (TPFB; **1**) and tris(hexafluoroisopropyl)borate (THFIPB; **2**).[1] This new battery cell chemistry is based upon the dual intercalation of lithium and fluoride ions into graphite anodes and cathodes, respectively.[1] Amine and co-workers have developed 2-(pentafluorophenyl)tetrafluoro-1,3,2-benzodioxaborole (**3**) as an anion receptor for fluoride anions and demonstrated its effect on the dissociation of LiF.[2]

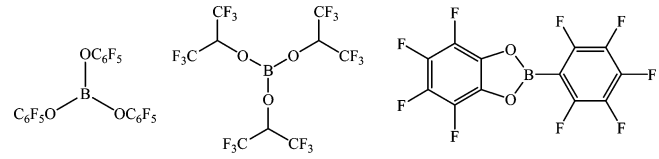

1 **2** **3**

Yang and McBreen and co-workers have shown that with TPFB (**1**) and THFIPB (**2**) and tris(pentafluorophenyl)borane (TPFPB), when used as anion receptors in LiF/carbonate electrolytes, lithium ion transference numbers could be realized as high as 0.7, and acceptable room-temperature ionic conductivity in the range of 10^{-3} Scm^{-1} was observed.[3−5] Solubility of the otherwise insoluble LiF also dramatically increased in the presence of these anion receptors.[2,3,6] The fluoride adducts of the anion receptors are also expected to provide a protective solid electrolyte interface (SEI) on the graphite surfaces, which should lead to improved capacity retention and power capability.[2,7,8] TPFB at relatively higher concentrations, however, significantly raises the interfacial impedance of lithium ion batteries.[9]

The optimal characteristics of the anion receptors for applications in high-specific-energy lithium ion batteries include their ability to sustain sufficiently high electrochemical windows, high solubilities, and diffusivities of their fluoride complexes and, more importantly, their fluoride anion affinities. The low affinity of fluoride anions to the receptors would not result in the sufficient

* To whom correspondence should be addressed. E-mail: preddy@mst.edu. Tel: (573)341-4768. Fax: (573)341-6033 (V.P.R.).
[†] Missouri University of Science and Technology.
[‡] Department of Chemistry, California Institute of Technology.
[§] Jet Propulsion Laboratory, California Institute of Technology.
[⊥] City University of New York.

10.1021/jp901952t CCC: $40.75 © 2009 American Chemical Society
Published on Web 04/27/2009

dissolution of LiF into the electrolyte solvents, while at the same time, too strong fluoride anion binding to the anion receptor would not efficiently release the bound fluoride anions during charging with resultant co-intercalation into the graphite cathodes.[1]

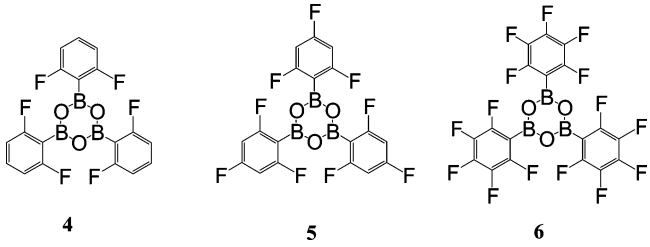

4 5 6

Here, we disclose our results on the effect of fluorinated boroxines, tris(2,6-difluorophenyl)boroxin (DF; **4**), tris-(2,4,6)trifluorophenylboroxin (TF; **5**), and tris(pentafluorophenyl)boroxin (PF; **6**) as novel anion receptors for potential applications in lithium ion batteries, through ab initio theory, fluoride anion binding studies, and ionic conductivities. These cyclic fluorinated boroxines have additional advantages as their Lewis acidity could be readily modulated by varying the number of fluorines on the aromatic rings. Our density functional theory (DFT) calculations substantiate this hypothesis and serve as a predictive tool for identifying the optimal anion receptors.

Experimental Methods Section

Materials. Acetonitrile (anhydrous, >99.8%), dimethylsulfoxide (>99.6%), dichloromethane (>99.8%), ethyl acetate (>99.5%), and tetrabutylammonium fluoride hydrate (>98%) were obtained from Aldrich and used as received. The fluorinated boroxines DF (**4**), TF (**5**), and PF (**6**) were obtained by thermal dehydration of the corresponding arylboronic acids at 100 °C for about one hour.[10] The products were obtained essentially pure as confirmed by their ^{19}F NMR and ^{11}B NMR spectra (vide infra). Further confirmation of the structures was provided by matching the observed chemical shifts with those obtained at the GIAO/B3LYP/6-31G** level.[11]

NMR Spectra. ^{19}F NMR spectra (at 376 MHz) and ^{11}B NMR spectra (128 Hz) were obtained on a Varian Inova 400 MHz spectrometer in anhydrous CH_3CN (in unlocked mode) or CD_3CN solutions. ^{19}F NMR spectra were referenced to $CFCl_3$ ($\delta^{19}F = 0$), and ^{11}B NMR spectra were referenced to BF_3-OEt_2 ($\delta^{11}B = 0$).

A series of solutions (about 200 mM) of boroxines (DF, TF, and PF) were prepared by dissolving each of the boroxines in various solvents (acetonitrile, DMSO, ethyl acetate, and dichloromethane), and appropriate amounts of tetrabutylammonium fluoride (TBAF) were added to them so that the resulting solutions had mole ratios of boroxine/fluoride of 1:0, 1:1, 1:2, and 1:3. These homogeneous solutions were transferred into 5 mm NMR tubes, $CFCl_3$ was added as an internal reference, and ^{19}F NMR spectra were recorded at ambient temperature. ^{11}B NMR spectra were obtained for the same solutions using BF_3-etherate as the external reference.

The reaction of boroxines (DF, TF, and PF) with the fluoride anion was exothermic. A clear homogeneous solution resulted immediately after the addition of TBAF to DF and TF. However, reaction of PF with TBAF gave homogeneous solutions only in DMSO, acetonitrile, and dichloromethane, but not in ethyl acetate. The ^{11}B and ^{19}F NMR spectra for the boroxines and their fluoride complexes **7**, **8**, and **9** (1:1 mol ratio) in acetontrile are as follows:

DF: δ^{19}F, −103.0 (broad s); δ^{11}B, 28.5.

TF: δ^{19}F, −99.9 (apparent triplet, $J = 7.5$ Hz, *ortho*-F), 106.8 (t, $J = 8$ Hz; *para*-F); δ^{11}B, 28.0.

PF: δ^{19}F, −132.4 (m, *ortho*-F), −153.7 (t, $J = 19$ Hz, *para*-F), −163.5 (m, *meta*-F). δ^{11}B, 27.3 (broad s), 20.4 (broad s).

Complex **7**: δ^{19}F, −110.4 (broad s, *ortho*-F); (additional small peaks, δ^{19}F, −102 to −105, were observed, presumably corresponding to multiple fluoride exchange equilibria); δ^{11}B, 28.5 (broad s), 20.4 (broad s), 3.0 (m).

Complex **8**: δ^{19}F, −107.9 (m, *ortho*- and *para*-F) (additional small peaks, δ^{19}F, −98 to −115, were observed, presumably corresponding to multiple fluoride exchange equilibria); δ^{11}B, 28.0 (broad s), 20.1 (broad s), 2.8 (m).

Complex **9**: PF: δ^{19}F, −139.3 (m, *ortho*-F), −155.3 (t, *para*-F), −162.9 (m, *meta*-F). δ^{11}B, 20.4(broad s), 1.95 (broad s), 1.2 (m).

Addition of 2 mol equiv of TBAF simplified the ^{19}F NMR spectra of the complexes **7** and **8**. There was no apparent change in the spectra of complex **9**. The δ^{19}F remained constant upon further addition of up to 3 mol equiv of TBAF to each of these complexes (**7**, **8**, and **9**). The ^{19}F and ^{11}B NMR spectra of these complexes with 2 mol equiv of fluoride anion are as follows

Complex **7** (with excess TBAF): δ^{19}F, −110.4 (broad s); δ^{11}B, 20.4 (broad s), 1.2 (broad s).

Complex **8** (with excess TBAF): δ^{19}F, −107.9 (m, *ortho*- and *para*-F); δ^{11}B, 20.4, 1.2.

Complex **9** (with excess TBAF): δ^{19}F PF: δ^{19}F, −139.3 (m, *ortho*-F), −155.3 (t, $J = 19$ Hz, *para*-F), −162.9 (m, *meta*-F); δ^{11}B, 20.4 (broad s), 1.2 (broad s).

UV−Vis Spectroscopic Studies. UV−vis spectroscopic studies were carried out on a Cary-50 UV−vis spectrophotometer equipped with a 1 cm path length quartz cell by monitoring the absorbances between 200 and 300 nm. Micropipets used were capable of delivering 1 mL solutions, having adjustable ranges between 100 and 1000 μL. All UV−vis measurements were performed at ambient temperature. Stock solutions (1×10^{-5} M) of DF (**4**), PF (**6**), and tetrabutylammonium fluoride (TBAF) were prepared in acetonitrile. The stoichiometry of the DF−fluoride (PF−fluoride) complexes was determined using Job's continuous variation method as follows.

A series of solutions consisting of DF (PF) and TBAF were prepared by mixing the above stock solutions so that the total concentration of the combined solutions was maintained constant at 1×10^{-5} M, and the UV absorbances were recorded separately for each solution. The stoichiometry of the complexes was determined by a plot of the absorbances (multiplied by the mol fraction of boroxines) versus mol fractions of the TBAF.

Ab Initio Calculations. We conducted thermodynamic calculations, in the form of electronic energies, solvation free energies in propylene carbonate, and binding energetics using quantum mechanical density functional theory (B3LYP)[12] for reactions of the fluoride anion binding to novel fluorinated phenyl boroxin anion receptors. We performed full geometry optimizations with solvation effects obtained through a continuum dielectric model.[13] The molecular solvation surface of the anion receptor was defined with the molecular radius (2.7Å) and dielectric constant of propylene carbonate ($\varepsilon = 64.5$). All wave functions are open shell (UDFT), calculated with a high-level basis set (LACVP**) which translates to the 6-311 G** basis for main group elements. Ab initio calculations were carried out on a Dell Linux Cluster (80 node/160 core, Single Core Xeon, 3.06 GHz) running Linux/OSCAR, with 160 GB of RAM and 8.6 TB of disk space. ^{11}B and ^{19}F NMR chemical shifts were calculated using density functional theory, at the B3LYP/6-311G** level, for the various fluorinated receptors and fluoride complexed anions. The geometries were fully

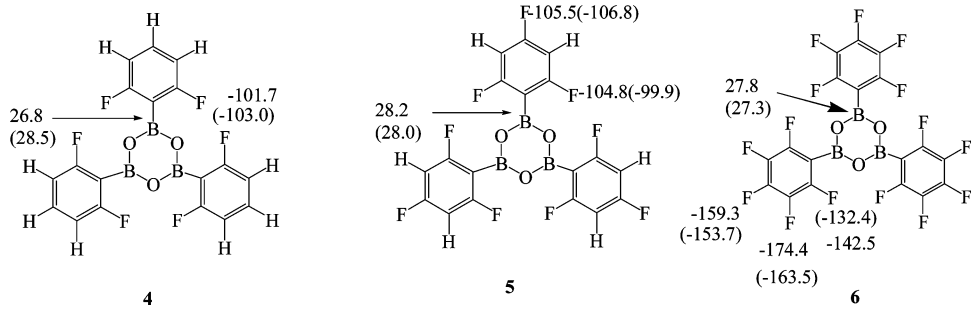

4 5 6

Figure 1. Experimental (acetonitrile solvent; in parentheses) and GIAO/B3LYP/6-31G** calculated δ^{19}F ($\delta CFCl_3 = 0$) and ^{11}B NMR spectra for DF, TF, and PF; δ^{11}B are shown using arrows ($\delta BF_3 \cdot OEt_2 = 0$).

optimized (basis set 6-311G**) in a continuum dielectric medium appropriate for propylene carbonate (PC). The ^{19}F and ^{11}B NMR chemical shifts were computed with respect to $CFCl_3$ ($\delta^{19}F = 0.0$) and BF_4^- ($\delta^{11}B = 0.0$), respectively. The latter $\delta^{11}B(BF_4^-)$ were reconverted to $\delta^{11}B(BF_3 \cdot Et_2O)$ ($\delta^{11}B(BF_4^-) = -2.2$ with respect to $\delta^{11}B(BF_3 \cdot OEt_2$; $\delta^{11}B = 0$).

Lithium Ion Conductivities. A series of 0.1 M boroxine-based anion receptors dissolved along with LiF in propylene carbonate (PC) were prepared using an excess of LiF relative to the anion receptor (0.1 M anion receptor + 0.2 M LiF) in order to probe for the fluoride anion binding. The ionic conductivities of these solutions were measured using a Pt/Pt conductivity cell through electrochemical impedance spectroscopy, calibrated with standard commercially available samples.

Results and Discussion

Boron-based anion receptors such as tris(pentafluorophenyl)borane have recently been used for selective binding of fluoride anions in lithium ion batteries.[2,5,8,14] In order to systematically fine-tune the binding efficiencies of the boron-based anion receptors, we have now synthesized a series of fluorinated arylboroxines—DF (**4**), TF (**5**), and PF (**6**)—by thermal dehydrative cyclizations of the corresponding arylboronic acids. These boroxines are novel compounds and have not been used in lithium ion battery applications. The structures of these compounds were readiy assigned based on ^{19}F and ^{11}B NMR spectra, which closely match with those calculated by ab initio theory (Figure 1). ^{11}B NMR are especially diagnostic of the structures as deviations of the experimental chemical shifts from GIAO/B3LYP-6-31G** derived values are too small, $\Delta\delta = 1.7$ (DF), 0.2 (TF), 0.5 (PF).

The synthetic method adapted is comparatively simple and allows synthesis of a wide variety of fluorinated boroxines from their corresonding arylboronic acids.[10,15,16] Further, the binding efficiencies of these boroxines can be readily optimized by tailoring the degree of fluorination on the aryl rings or by incorporating additional electron-withdrawing groups. These anion receptors could be readily monitored for their anion binding efficiency using ^{19}F and ^{11}B NMR spectroscopy. We have explored the ionic conductivities, fluoride anion binding efficiencies, and binding stoichiometries of these boroxines. These results are further substantiated by ab initio theoretical calculations.

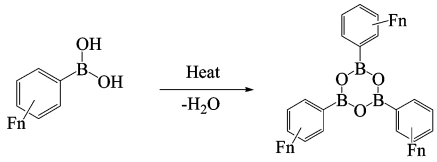

(1)

DF (4); TF (5); PF (6)

Structural Characterization. The boroxines **4**−**6** were characterized by ^{19}F and ^{11}B NMR spectroscopy, and the structures were confirmed through comparison of the chemical shifts with those obtained by the ab initio GIAO/B3LYP/6-31G**[11] method (Figure 1). The ^{19}F NMR spectrum for DF (**4**) showed a single absorption at −103.0 ppm, which is very close to the GIAO/B3LYP/6-31G** of −101.7 ($\Delta\delta = 1.3$). TF (**5**) showed two ^{19}F absorptions at δ^{19}F −99.9 (*ortho*-F) and −106.8 (*para*-F), agreeing with those of DFT-GIAO calculations, −104.8 (*ortho*-F, $\Delta\delta = 4.82$) and −105.5 (*para*-F, $\Delta\delta = 2.34$). PF (**6**) showed three absorptions at −132.4 (*ortho*-F), −153.7 (*para*-F), and −163.0 (*meta*-F). The *ortho*-, *meta*-, and *para*-fluorine assignments are supported by the ab initio calculated chemical shifts, although the theoretically obtained chemical shifts deviate from the experimental values by 6−10 ppm. Further, the ^{11}B NMR spectra closely match the experimental values for DF ($\Delta\delta = 1.7$), TF ($\Delta\delta = 0.2$), and PF ($\Delta\delta = 0.5$), showing that the GIAO ^{11}B NMR chemical shifts are reliable indicators of the structural characterization of the boroxines.[17,18]

Solvation Effects. It has been established through X-ray diffraction studies that tris(pentafluorophenylborane) can form 1:1 adducts with solvents such as acetonitrile.[19] In order to see similar solvation effects on fluorinated boroxines, we have explored the effect of solvents on the stabilization of the boron centers through ^{19}F NMR spectroscopy (Figure 2). In the relatively non-nucleophilic solvent, dichloromethane, DF shows a single absorption at δ^{19}F −104.5, whereas in acetonitrile, dimethylsulfoxide, and ethyl acetate, the absorption has shifted downfield by 1 ppm to −103. It shows a significant solvation effect from these solvents. Similarly, for TF, $\delta^{19}F(CH_2Cl_2)$ signals at −101.1(*ortho*-F) and −103.2 (*para*-F) are shifted downfield by 1 ppm for the *ortho*-fluorine, and *para*-fluorine is shifted by 4 ppm upfield in DMSO, acetonitrile, and ethyl acetate.

On the other hand, PF (**6**) shows relatively more sensitivity to solvation effects. In the more coordinating DMSO solvent, the $\delta^{19}F$ (CH_2Cl_2) signals at −132.8 (*ortho*-F), −149.6 (*para*-F), and −161.5 (*meta*-F) are split into multiple peaks from −131 to −164 ppm in DMSO, indicating the formation of stable PF−DMSO adducts. In acetonitrile and ethyl acetate solvents, the $\delta^{19}F(CH_2Cl_2)$ absorptions are shifted downfield by 0.5 ppm for *ortho*-fluorines, upfield by 5 ppm for *para*-fluorines, and upfield by 2 ppm for the *meta*-fluorines.

The ^{19}F NMR of PF, TF, and DF in various solvents thus clearly show the importance of solvation. In the cases of TF and DF, there is rapid exchange of the solvent molecules among the three boron centers of the complex, so that only a single ^{19}F NMR absorption is observed for all of the aromatic *ortho*- or *para*-fluorines. However, in relatively more polar DMSO solvent, additional distinct absorptions for PF−DMSO adducts

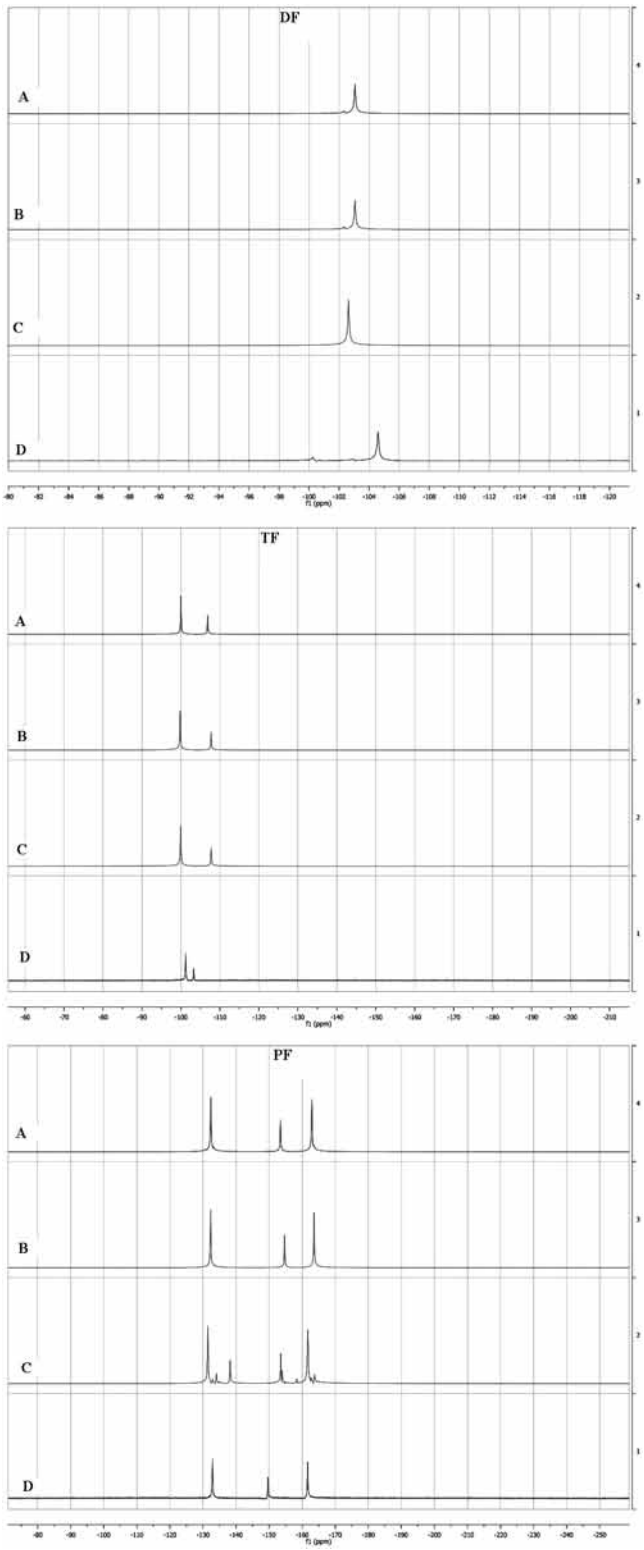

Figure 2. ^{19}F NMR spectra of DF (**4**), TF (**5**), and PF (**6**) in CH_3CN (A), EtOAc (B), DMSO (C), and CH_2Cl_2 (D).

could be observed. This indicates relatively slow exchange of the DMSO with PF. Unlike the starting boroxines, the boroxine−fluoride adducts (in the presence of excess fluoride anion) have similar $\delta^{19}F$ in all of the solvents studied (CH_2Cl_2, acetonitrile, and DMSO), showing that the solvent participation is minimal in the case of the fluoride adducts.

Fluoride Anion Binding. Fluoride anion binding to anion receptors not only helps the solubility of the otherwise insoluble lithium fluoride electrolyte in nonaqueous organic solvents but also dramatically increases the lithium ion conductivities. Reversibility of fluoride anion binding is crucial in the next generation dual ion intercalating lithium ion batteries. In order to understand the structural effects on the fluoride binding to anion receptors, we carried out DFT calculations on a series of fluorinated boroxines, and the results are shown in Table 1 and Figure 3. As can be seen from Figure 3, fluoride anion binding is correlated with the number of the fluorines on the aryl rings; the more fluorines in the aryl rings, the higher the binding efficiency of the boronic anhydrides (boroxines). Because there is more than one boron capable of anion capture, we estimated the binding energies for the second and third fluoride and report the data in Table 1. These calculations are less reliable because they involved highly charged species. Nonetheless, it appears that multiple bindings are favorable (exothermic). Second and third anion binding energies do not follow the same trend as a function of fluorination that the first anion binding follows.

To understand the binding abilities of the fluorinated boroxines with the fluoride anion, we have carried out ^{19}F NMR spectroscopic studies for solutions of boroxines with varied amounts of TBAF. A series of samples of boroxines (**4**−**6**) were prepared in acetonitrile, dichloromethane, and DMSO and contained 0, 1, 2, and 3 equiv of TBAF and $CFCl_3$ ($\delta CFCl_3$ = 0) as the internal reference, and the spectra were recorded in the unlocked mode. The ^{19}F and ^{11}B NMR spectra of the boroxin−fluoride complexes (**7**−**9**) in acetonitrile are summarized in Figure 5. The DF−fluoride complex, **7** (with 2 equiv of TBAF), shows a single absorption, $\delta^{19}F$ −110.4 (*ortho*-F). The TF−fluoride complex, **8** (with 2 equiv of TBAF), also shows only a single ^{19}F absorption at −107.9 ppm due to the coincidental merging of the *ortho*- and *para*-fluorines; that is, the *ortho*-fluorines are shielded much farther than the *para*-fluorine with respect to the corresponding neutral boroxin. The PF-fluoride complex, **9** (with 1 or 2 equiv of TBAF), shows three ^{19}F absorptions at −139.3 (*ortho*-F), −155.3 (*meta*-F), and −162.9 (*para*-F).

The assignments of the chemical shifts of these boroxin−fluoride complexes, **7**, **8**, and **9**, could be readily confirmed through their DFT-GIAO chemical shifts (Figure 4). The DFT-GIAO derived $\delta^{19}F$ for the *ortho*-fluorines in these complexes vary slightly from each other, whereas they show single absorptions in solution NMR, indicating rapid rotation across the B-aryl bonds in the solution phase. Further, the DFT values also reflect different chemical environments for the two sets of aryl groups. In solution, due to the rapid intramolecular exchange of the fluoride anion among the three borons, a single $\delta^{19}F$ absorption is observed (vide infra). The DFT-GIAO predicts a $\delta^{19}F$ of −166.7, −168.8, and −164.6 for the B−F fluorine in structures **7**, **8**, and **9**, respectively. These absorptions could not be observed in solution, perhaps due to the rapid intramolecular fluoride anion exchange (vide infra).

Upon addition of 1 mol equiv of TBAF to PF (**6**), in acetonitrile solvent, complete disappearance of the ^{19}F NMR peaks for the starting material was observed, and a three line ^{19}F NMR spectrum for the PF−fluoride complex, **9**, was observed; $\delta^{19}F$ −139.3, −155.3, −162.9 (Figure 5). However, for DF (**4**) and TF (**5**), upon addition of 1 mol equiv of TBAF, a complex spectrum resulted with multiple absorptions corresponding to the boroxin−fluoride complexes (**7** and **8**), presumably because of their equilibration with unreacted boroxines. Addition of 2 mol equiv of TBAF to these solutions resulted in surprisingly simplified spectra showing only one absorption (less than 0.1% of the starting material could be observed by ^{19}F NMR). These results show that PF has relatively stronger

TABLE 1: Fluoride (F^-) Anion Binding Energies (B3LYP, LACVP), Solvation Energies, and Degree of Fluorination for Various Fluorinated Arylboroxines[a]**

compound	degree of fluorination	binding energy (kcal/mol)
tris(pentafluorophenyl)boroxin (**6**)	15	74.1
(2,6-difluorophenyl)-bis(pentafluorophenyl*)boroxin	12	73.1
bis(2,6-difluorophenyl)-(pentafluorophenyl*)boroxin	9	71.0
bis(2,6-difluorophenyl*)-(pentafluorophenyl)boroxin	9	70.0
tris(2,4,6-trifluorophenyl)boroxin (**5**)	9	69.3
tris(2,6-difluorophenyl)boroxin (**4**)	6	67.5
tris(4-fluorophenyl)boroxin	3	61.6
Second Anion Captured		
(2,6-difluorophenyl)-bis(pentafluorophenyl**)boroxin	13	49.1
bis(2,6-difluorophenyl*)-(pentafluorophenyl*)boroxin	10	45.9
Third Anion Captured		
(2,6-difluorophenyl*)-bis(pentafluorophenyl**)boroxin	14	16.6
bis(2,6-difluorophenyl*)-(pentafluorophenyl**)boroxin	11	11.2

[a] The * indicates the location of fluoride anion binding.

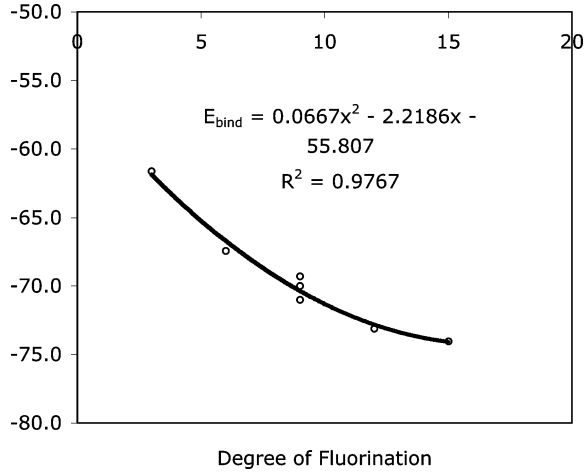

Figure 3. Effect of the degree of aryl fluorination on the fluoride anion binding energies (kcal/mol) from DFT (B3LYP).

fluoride affinity as compared to DF and TF. The data in Table 1 are also in accordance with these results; that is, the higher the aryl-fluorination, the stronger the fluoride binding.

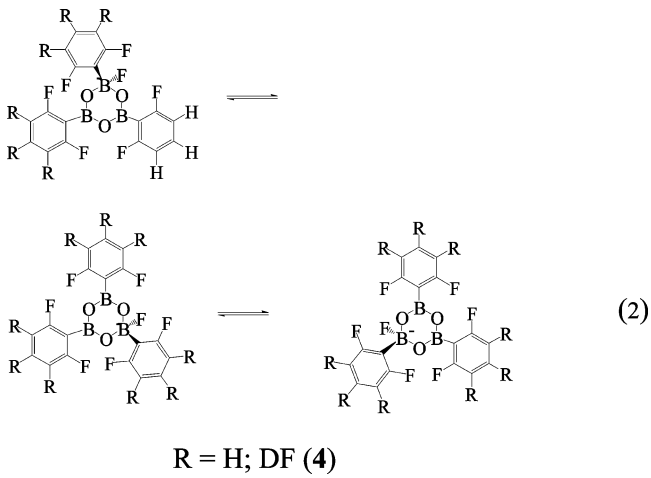

(2)

At first glance, we would have expected distinct ^{19}F absorptions for the two sets of aromatic rings for complexes **7**−**9**; that is, the aryl rings bound to sp^3-hybridized boron are chemically different than those attached to sp^2-hybridized boron. The observation of a single *ortho*-^{19}F (or *para*-^{19}F) absoption for each of these complexes (with excess fluoride in case of DF and TF) shows that there is a rapid intramolecular fluoride exchange between the three borons (eq 2) with an upper limit of free energy of activation of 12.5, 12.4, and 12.0 kcal/mol for boroxin−fluoride complexes **7**, **8**, and **9**, respectively (corresonding to exchange rate constants of 4400, 4800, and 9200 s^{-1}, respectively).[20] Presumably due to this low barrier for exchange, the $\delta^{19}F$ for B−F fluorine could not be observed in solution (vide supra).

Anion receptor PF (**6**), in acetonitrile, in the presence of 1 mol equiv of fluoride showed three new absorptions at −139.3 (*ortho*-F), −155.3 (*para*-F), and −162.9 (*meta*-F) corresponding to the PF−fluoride complex, and the absorptions for PF completely disappeared (Figure 5). Further addition of TBAF (2−3 mol equiv) resulted in no change of the spectra, showing that the stoichiometry of the PF−fluoride complex is 1:1. The formation of the fluoride complex is essentially irreversible as the absorptions corresonding to the starting PF could not be observed even after addition of 1 mol equiv of TBAF. The *ortho*-fluorines are relatively more shielded in the PF−fluoride complex (**9**) as compared to the *meta*- and *para*-fluorines, as expected due to the proximity of the negatively charged boron.

^{11}B NMR Studies. The ^{11}B NMR for the fluoride complexes (**7**, **8**, and **9**) are shown in Figure 5. The DF−fluoride complex (**7**) shows two ^{11}B absorptions at $\delta^{11}B$ 19.8 (sp^2-B) and 1.2 (sp^3-B). The TF−fluoride and PF−fluoride complexes similarly show two ^{11}B absorptions at $\delta^{11}B$ (TF), 20.1 (sp^2-B) and 1.2 (sp^3-B), and $\delta^{11}B$ (PF), 20.4 (sp^2-B) and 1.2 (sp^3-B). The DFT-GIAO derived chemical shifts are in reasonably close agreement ($\Delta\delta$ = 2.8−5.9) with experimental values; therefore, the assignments of the ^{11}B absorptions in the complexes can be confirmed. In the presence of 1 mol equiv of TBAF, about 20% of the unreacted starting materials could be observed in the case of DF and TF, in addition to the above two ^{11}B absorptions for the fluoride complexes, **7** and **8**, showng their equilibration with residual boroxines. Further, the chemical shifts of the sp^3-hybridized boron in complexes **7** and **8** is shielded by 2 ppm in the presence of 2 equiv of TBAF, presumably due to the weak binding of the second fluoride anion to these complexes.

Addition of 1 mol equiv of TBAF to PF, however, resulted in instantaneous complete disappearance of the starting material as monitored by ^{11}B NMR spectroscopy. The PF−fluoride complex, **9**, showed three relatively broad signals at $\delta^{11}B$ 20.4 (sp^2-B), 2.2 (sp^3-B), and 1.4 (sp^3-B) (Figure 5). Further addition of TBAF to this solution resulted in gradual broadening of the peak at 2.2 ppm. Although we cannot clearly rationalize this

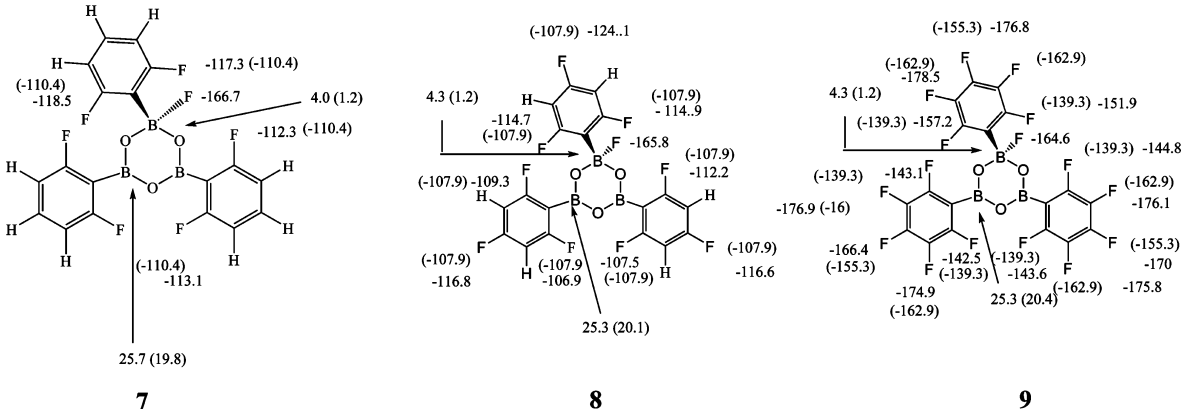

7 **8** **9**

Figure 4. Experimental (acetonitrile solvent; δ^{19}F in parentheses) and GIAO/B3LYP/6-31G** calculated δ^{19}F ($\delta CFCl_3 = 0$) for the boroxine−fluoride complexes (**7**−**9**); δ^{11}B are shown using arrows ($\delta BF_3 \cdot OEt_2 = 0$).

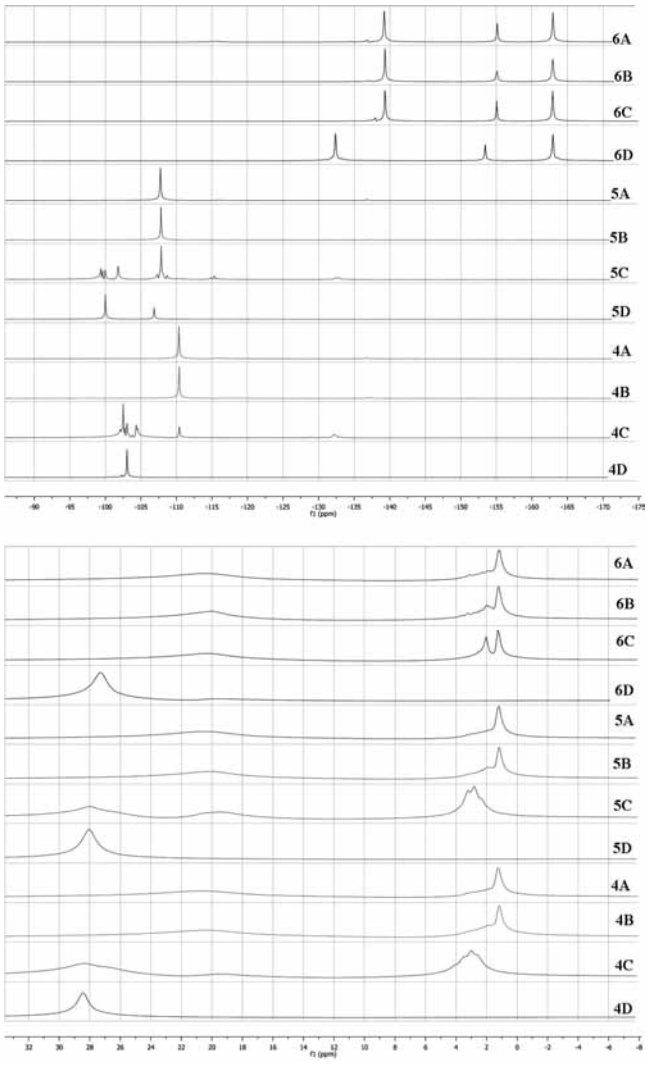

Figure 5. ^{19}F (top) and ^{11}B (bottom) NMR spectra of DF (**4**), TF (**5**), and PF (**6**) in acetonitrile at various molar equivalents of TBAF; boroxin/TBAF = 1:3 (A); boroxin/TBAF = 1:2 (B); boroxin/TBAF = 1:1 (C); boroxin without added TBAF (D).

unexpected observation for PF, perhaps a second fluoride anion binding may be involved in this case. In accordance with this expectation, UV−vis studies also show possible existence of multiple equilibria, that is, coexistence of more than one PF−fluoride complex (vide infra). Upon further addition of up to 3 mol equiv of TBAF, the spectra for boroxin−fluoride complexes **7**, **8**, and **9** remained unchanged.

UV−Vis Studies. UV−vis spectroscopy is commonly used to identify the stoichiometry of host−guest complexes.[21] In order to further confirm the ^{19}F NMR derived stoichiometry for the boroxine−fluoride complexes, we have carried out UV−vis studies for these complexes using continuous variation method (Job's plots).

UV−vis spectra were recorded for a series of DF/TBAF (PF/TBAF) solutions; the mole ratios of DF to fluoride (PF to fluoride) were continually varied while keeping the total concentration of each of their solutions constant. The measured UV−vis absorbances at 265, 265, 260, and 254 nm (multiplied by the mole fraction of boroxines) were plotted against mole fractions of the TBAF (Figure 6).[22,23] Through these Job's plots, the stoichiometry of the DF−fluoride complex was determined as 1:1. In the case of DF, the 1:1 stoichiometry is consistently observed at all wavelengths, 269, 265, 260, and 254 nm (Figure 6B). The stoichiometry of host−guest complexation is independent of the UV−vis wavelength in Job's plots if a single complex is formed. On the other hand, the dependence of Job's maxima on wavelength is indicative of the coexistence of more than one complex.[21,24,25] The Job's plots for PF, on the other hand, show deviations from 1:1 stoichiometry at different wavelengths, indicating the possibility of coexistence of more than one complex for PF (Figure 6C) (vide supra).

Ab Intio Structures of Boroxin−Fluoride Complexes. We have optimized structures of symmetrically bound and unsymmetrically bound fluoride anion complexes of DF at the B3LYP/6-31G** level in order to clarify the nature of the fluoride anion binding to the cyclic boroxines. Aldridge and co-workers have earlier shown that a related triboramacrocyclic compound, 1,4,7-trifloro-1,4,7-triboracyclononane (**11**) and its perfluorinated analogue have symmetrical fluoride anion binding to all three boron atoms at the HF/6-31+G* level.[26]

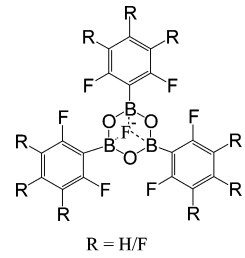

10

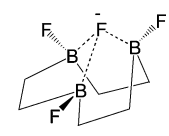

11

However, we have found at higher DFT levels of calculations at B3LYP/6-311G** that the symmetyrical C_{3v} structure for the

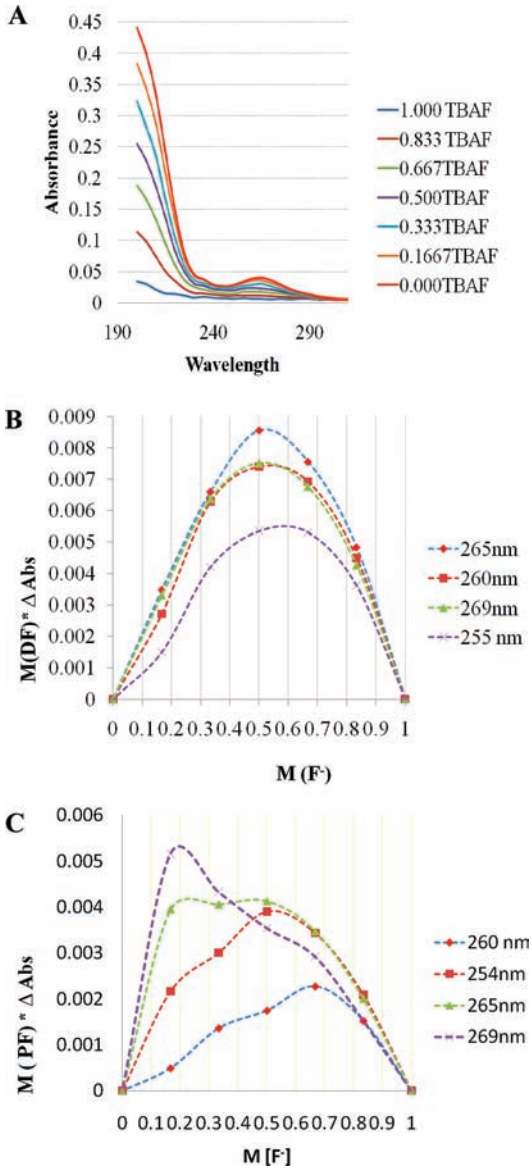

Figure 6. UV−vis spectra (in acetonitrile) obtained from the continuous variation method (A) and Job's plots for DF (B) and PF (C); B and C are the overlay plots for absorbances at 269, 265, 260, and 255 nm.

complex, **10**, is relatively 12.5 kcal/mol higher in energy as compared to that of the unsymmetrically bound species, **7**. Structures **7** and **10** are energy minima on the potential energy surface at this level of theory (Figure 7).

The relatively low energy for the unsymmetric structure (**7**) implies its entropic advantage over the symmetric structure, **10**. The fluoride bound complex, **7**, shows significantly upfield shifted ^{19}F signals for the fluorine atoms attached to aromatic rings. However, we were not able to observe the absorptions corresponding to the fluoride anion attached to boron. The lack of detection of the boron-bound fluoride absorption indicates that there is rapid equilibrium between three unsymmetrical structures relative to the NMR time scale at ambient temperature with an estimated free energy of activation of 12.0−12.5 kcal/mol (vide supra). Geometries for the PF and $[PF-F]^-$ are shown in Figure 8. In the neutral form, the PF anion receptor is a propeller-shaped molecule with a small angle (36.4°) between the boroxine ring and the phenyl groups. In the charged state $[PF-F]^-$, the boron atom that captures the fluoride anion

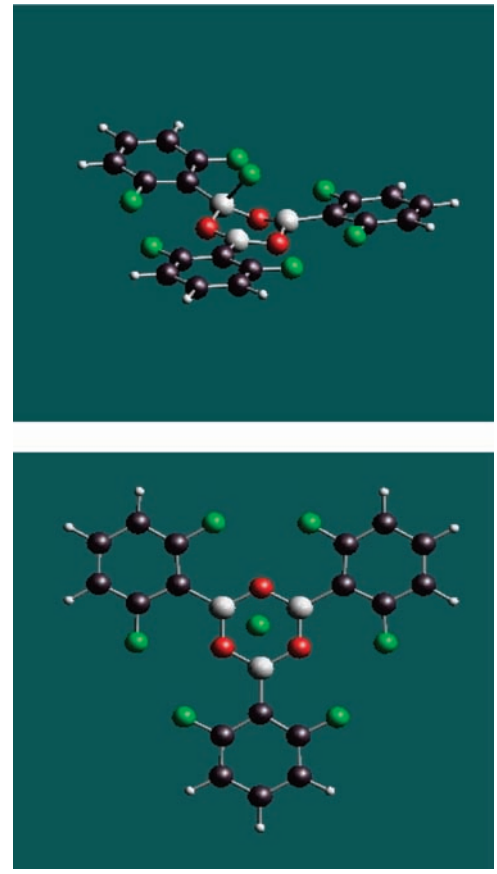

Figure 7. B3LYP/6-311G** structures of asymmetic and symmetrically bridged $[DF-F]^-$ complexes, corresonding to structures **7** (left) and **10** (right).

becomes more tetragonal, and the propeller angle increases significantly (79.7°).

Lithium Ion Conductivities. The lithium ion conductivities of the fluorinated boroxin (**4**, **5**, and **6**) solutions are estimated as near 0.5 mS/cm (Figure 9). The relative conductivities of these solutions are in the following order: PF (**6**) > DF (**4**) > TF (**5**). As a means of comparison, the conductivity of a solution using the well-known tris(pentafluorophenyl)borane (TPFPB)[5,8,14] yields virtually similar ionic conductivity as the PF solution with the same molarity. While the fluorinated boroxin/LiF ratio of the samples was 1:2, visual examination of the solution indicated that not all of the LiF was dissolved in the solution, and some fluorinated boroxin may also be insoluble at these molarities. On the basis of the observation that the ionic conductivity of the fluorinated boroxin/LiF did not exceed that of TPFPB/LiF, which is known to form 1:1 complexes, we conclude that the fluorinated boroxin/LiF ratio did not exceed 1:1. The solubility of all of the fluorinated boroxines in propylene carbonate is qualitatively lower than TPFPB, which necessarily limits the conductivity of the solutions.

It should be noted that the conductivity of perfluorinated boroxin (**6**) is significantly higher than that the difluorinated or trifluorinated boroxines (**4** and **5**). Although there is no clear-cut correlation of conductivities with electron-withdrawing substituents, these studies show that the highly fluorinated boroxines show significant effect on the dissociation of LiF and thereby their increased conductivities. However, the lithium ion conductivities of these solutions are nearly 10 times smaller than those for 1 M $LiPF_6$ in PC, which signifies that even better anion receptors are needed to achieve relatively higher conductivities.

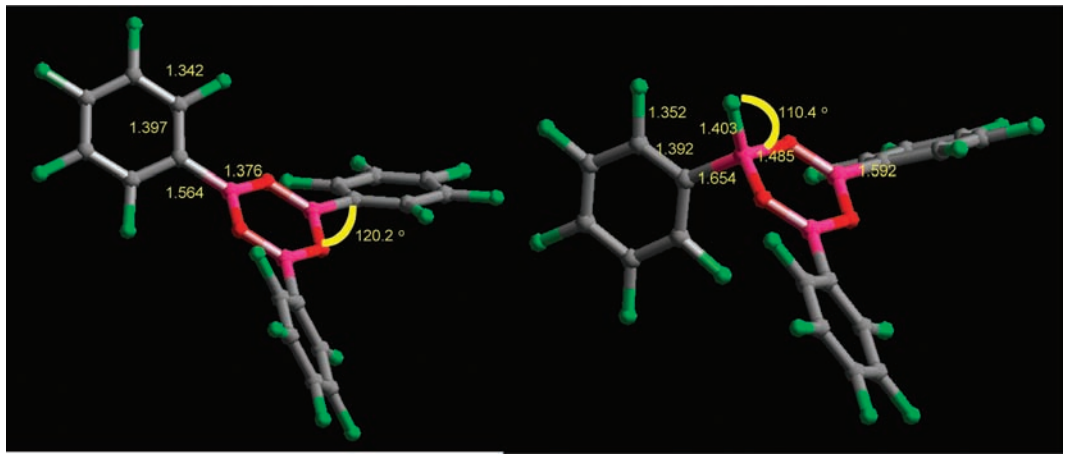

Figure 8. B3LYP/6-311G** solution (propylene carbonate) geometry-optimized structures of neutral PF (left) and the corresponding charged $[PF-F]^-$ complex (right).

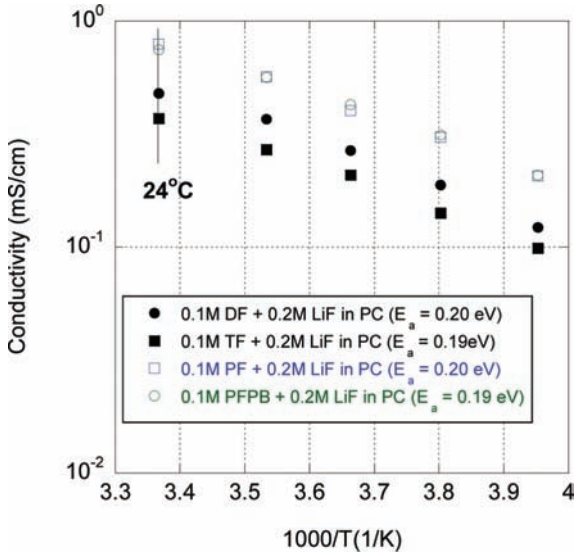

Figure 9. Conductivity of anion receptor−salt solutions in propylene carbonate (PC) as a function of temperature.

We have also measured lithium diffusivities by ^{7}Li NMR for the solutions of LiF in boroxines, **4**−**6**, and PFPB, which ranged from 1.88 to 2.12 × 10^{-6} cm^2/sec. The latter diffusivity is relatively higher than the reported value for Li^+/propylene carbonate (1.5 × 10^{-6} cm^2/sec).[27] The discrepancy shows the relatively reduced association of Li^+ with the boroxines and PFPB, which is also in accord with high lithium ion conductivities in the presence of boroxines (Figure 9).

Conclusion

In summary, fluorinated arylboroxines are efficient anion receptors, comparable to the state of the art PFPB anion receptor.[8,14,19] The structures of the fluoride complexes DF, TF, and PF are confirmed by matching the experimental ^{19}F and ^{11}B NMR chemical shifts with those obtained from DFT calculations.

Our ab initio calculations show that the symmetrically bound fluoride complex, **10**, is, unexpectedly, less favorable as compared to the unsymmetrically bound species, **7**, by 12.5 kcal/mol. The coalescence of the ^{19}F NMR signals of these boroxines at ambient temperature shows relatively rapid equilibration of the fluoride anion among the three boron atoms in these boroxines, with an estimated upper limit of about 12 kcal/mol.

Acknowledgment. The work described here was carried out, in part, at the Jet Propulsion Laboratory, California Institute of Technology, under contract with the National Aeronautics and Space Administration. Authors W.C.W. and M.B. gratefully acknowledge the support of this work by the Army Research Office. N.G.N. gratefully acknowledges graduate fellowship from Missouri S&T.

References and Notes

(1) West, W. C.; Whitacre, J. F.; Leifer, N.; Greenbaum, S.; Smart, M.; Bugga, R.; Blanco, M.; Narayanan, S. R. *J. Electrochem. Soc.* **2007**, *154*, A929–A936.
(2) Chen, Z.; Amine, K. *Electrochem. Commun.* **2007**, *9*, 703–707.
(3) McBreen, J.; Lee, H. S.; Yang, X. Q.; Sun, X. *J. Power Sources* **2000**, *89*, 163–167.
(4) Li, L. F.; Lee, H. S.; Li, H.; Yang, X. Q.; Nam, K. W.; Yoon, W. S.; McBreen, J.; Huang, X. J. *J. Power Sources* **2008**, *184*, 517–521.
(5) Xie, B.; Lee, H. S.; Li, H.; Yang, X. Q.; McBreen, J.; Chen, L. Q. *Electrochem. Commun.* **2008**, *10*, 1195–1197.
(6) Choi, N.-S.; Ryu, S.-W.; Park, J.-K. *Electrochim. Acta* **2008**, *53*, 6575–6579.
(7) Chen, Z.; Liu, J.; Amine, K. *Electrochim. Acta* **2008**, *53*, 3267–3270.
(8) Sun, X.; Lee, H. S.; Yang, X.-Q.; McBreen, J. *Electrochem. Solid-State Lett.* **2003**, *6*, A43–A46.
(9) Chen, Z.; Amine, K. *J. Electrochem. Soc.* **2006**, *153*, A1221–A1225.
(10) Frohn, H. J.; Adonin, N. Y.; Bardin, V. V.; Starichenko, V. F. *Z. Anorg. Allg. Chem.* **2002**, *628*, 2827–2833.
(11) Cao, Y.; Beachy, M. D.; Braden, D. A.; Morrill, L.; Ringnalda, M. N.; Friesner, R. A. *J. Chem. Phys.* **2005**, *122*, 224116/224111–224116/224110.
(12) Becke, A. D. *J. Chem. Phys.* **1993**, *98*, 5648–5652.
(13) Tannor, D. J.; Marten, B.; Murphy, R.; Friesner, R. A.; Sitkoff, D.; Nicholls, A.; Honig, B.; Ringnalda, M.; Goddard, W. A. *J. Am. Chem. Soc.* **1994**, *116*, 11875–11882.
(14) Sun, X.; Lee, H. S.; Lee, S.; Yang, X. Q.; McBreen, J. *Electrochem. Solid-State Lett.* **1998**, *1*, 239–240.
(15) Zeng, H.; Hua, R. *J. Org. Chem.* **2008**, *73*, 558–562.
(16) Rambo, B. M.; Lavigne, J. J. *Chem. Mater.* **2007**, *19*, 3732–3739.
(17) Hong, D.; Carroll, P. J.; Sneddon, L. G. *J. Organomet. Chem.* **2003**, *680*, 61–65.
(18) Bluhm, M. E.; Bradley, M. G.; Butterick, R., III; Kusari, U.; Sneddon, L. G. *J. Am. Chem. Soc.* **2006**, *128*, 7748–7749.
(19) Jacobsen, H.; Berke, H.; Doering, S.; Kehr, G.; Erker, G.; Froehlich, R.; Meyer, O. *Organometallics* **1999**, *18*, 1724–1735.
(20) We have estimated the rate constant (k) of the fluoride exchange at ambient temperature using the equation $k = (\pi/\mathrm{sqrt2})\Delta\delta$, where $\Delta\delta$ is the separation of the corresponding ^{19}F signals at slow exchange limit (in hertz), obtained from the DFT-GIAO calculations, since the signal coalescence occurs well below ambient temperature. Symmetry-related DFT chemical shifts are averaged, and the difference in δ^{19}F of sp^3B-aryl and sp^2B-aryl *ortho*-fluorines is taken as $\Delta\delta$. Through this estimated exchange

rate constant, an upper limit of the activation barrier was calcaulted using the Eyring equation, $k = (k_B T/h)e^{-\Delta G^*/RT}$; (a) Sandstrom, J. *Dynamic NMR Spectroscopy*; Academic Press: New York, 1982; (b) Raban, M.; Kost, D.; Carlson, E. H. *J. Chem. Soc., Chem. Commun.* **1971**, *1913*, 1656.

(21) Connors, K. A. *Binding Constants: The Measurements of Molecular Complex Stability*; John Wiley: New York, 1987.

(22) Hirose, K. *J. Inclusion Phenom. Macrocyclic Chem.* **2001**, *39*, 193–209.

(23) Karikari, A. S.; Mather, B. D.; Long, T. E. *Biomacromolecules* **2007**, *8*, 302–308.

(24) Atkinson, G. F. *J. Chem. Educ.* **1974**, *51*, 792–798.

(25) Vosburgh, W. C.; Cooper, G. R. *J. Am. Chem. Soc.* **1941**, *63*, 437–442.

(26) Aldridge, S.; Fallis, I. A.; Howard, S. T. *Chem. Commun.* **2001**, 231–232.

(27) Hayamizu, K.; Aihara, Y. *Electrochim. Acta* **2004**, *49*, 3397–3402.

JP901952T